

# Implementation of a Microprocessor-based Sensorless Switched Reluctance Drive

Tian-Hua Liu and Yih-Hua Chang

Department of Electrical Engineering  
National Taiwan University of Science and Technology  
43 Keelung Road, Section 4,  
Taipei, Taiwan 106, R. O. C.  
E-mail: [Liu@mail.ntust.edu.tw](mailto:Liu@mail.ntust.edu.tw) and [cew@vip.url.com.tw](mailto:cew@vip.url.com.tw)

## Abstract

This paper presents a sensorless technique for a switched reluctance drive system. By measuring the induced voltage, the shaft position of the rotor position has been estimated. The adjustable speed range of the proposed drive system can vary from 30 r/min to 1500 r/min. The process by which a 32-bit microprocessor system is used to execute the position and speed estimation, speed-loop control, and current-commands generation is shown. Several experimental results validate the theoretical analysis. This paper presents a new direction in the design and implementation of a sensorless switched reluctance drive system.

## I. Introduction

Switched reluctance motor (SRM) drive technology has been developed over the last two decades. The SRM system has many advantages. For example, both the motor configuration and the power converter are simple and rugged. There is no winding in the rotor. As a result, the SRM has a higher efficiency than the induction motor [1]-[2]. The sensorless drive is a new direction in the design and implementation of the SRM drive system. Several papers on different sensorless techniques in this field have been published[3]-[4]. Recently, a sensorless method has been proposed by measuring a mutually induced voltage of an inactive phase of the SRM [5]. This is an effective way to estimate the shaft position of the SRM because it provides a clear relationship between the induced voltage and the rotor position. This method, unfortunately, has some disadvantages as well. First, this method requires the

-----  
This research is supported by the National Science Council, R. O. C., under grant NSC 89-2213-E-011-071.

design of a sample and hold circuit which is controlled by a synchronizing signal. The circuit, therefore, is difficult to implement. Second, after the sample and hold circuit, the mutually induced voltage is related to the current command, the stator resistance, the mutual inductance, the self-inductance, and the rotor speed of the switched reluctance motor. Moreover, this method can be used in the high frequency PWM region only. The proposed sensorless method in paper [5], therefore, has some limitations. For example, a three-dimensional table is required and the circuit is very complicated. One author of this paper proposed a method to solve the problem mentioned above [6]. This method, however, works well only when the converter is operated in the PWM region. If the speed of the motor is increased, the current waveform becomes a single pulse. Then, the mutually induced voltage technique can not be applied. This paper, therefore, presents another method to solve the problem. The details are discussed as follows.

## II. Sensorless Technique

### A. Sensorless Technique in the PWM Region

When the motor is operated at a low speed, the voltage of the SRM is operated in the pulse-width modulation (PWM) region. A circuit used to detect the mutually induced voltage of the stator winding, which is inactive and in front of the currently energized winding, was designed by one of the authors of this paper [6]. For example, if the b-phase is energized, the mutually induced voltage of the a-phase is detected to determine the commutation angle (time) of turning off the b-phase as well as turning on the c-phase. This principle can be easily applied while the c-phase or the a-phase is energized.

The induced voltage of the mutual inductance for an

SRM can be expressed as

$$v_m = d\lambda_m / dt \quad (1)$$

$$\lambda_m = L_m i \quad (2)$$

where  $v_m$  is the induced voltage,  $\lambda_m$  is the mutual flux-linkage,  $L_m$  is the mutual inductance, and  $i$  is the energized current. Substituting (2) into (1), we can obtain

$$v_m = L_m di / dt + \omega_e i d L_m / d \theta_e \quad (3)$$

where  $\omega_e$  is the electrical rotor velocity of the motor.

The energized voltage can be expressed as

$$\begin{aligned} v_{ph} &= i r + d \lambda_{ph} / dt \\ &= i r + L_s di / dt + \omega_e i d L_s / d \theta_e \end{aligned} \quad (4)$$

where  $v_{ph}$  is the energized phase voltage,  $r$  is the stator resistance,  $\lambda_{ph}$  is the self-induced flux, and  $L_s$  is the self-inductance. According to equation (4), we can easily obtain

$$di / dt = (1/L_s)(v_{ph} - i r - \omega_e i d L_s / d \theta_e) \quad (5)$$

After substituting equation (5) into equation (3), we can obtain

$$\begin{aligned} v_m &= (L_m / L_s)(v_{ph} - i r - \omega_e i d L_s / d \theta_e) \\ &\quad + \omega_e i d L_m / d \theta_e \end{aligned} \quad (6)$$

The induced voltage is related to the switching mode of the energized winding. Fig. 1 shows the configuration of one leg of the converter. Then, we discuss the operation of the adjacent energized phase in Fig. 1. While the power devices  $T_1$  and  $T_2$  are conducted, the stator winding is operated in a conduction mode. In this mode, the phase voltage  $v_{ph}$  of the measured winding is equal to the input dc supply voltage  $V_{dc}$ . The induced voltage, therefore, can be expressed as

$$\begin{aligned} v_{mc} &= (L_m / L_s)(V_{dc} - i r - \omega_e i d L_s / d \theta_e) \\ &\quad + \omega_e i d L_m / d \theta_e \end{aligned} \quad (7)$$

where  $v_{mc}$  is the mutually induced voltage while the adjacent phase is operated in a conduction mode. On the other hand, while the adjacent energized phase is operated in a free-wheeling mode, its power devices  $T_1$  and  $T_2$  are turned off. Then the diodes  $D_1$  and  $D_2$  are turned on immediately to maintain the current of the winding as a constant. Therefore, the phase voltage  $v_{ph}$  is equal to  $-V_{dc}$ . The induced voltage can be expressed as

$$\begin{aligned} v_{mf} &= (L_m / L_s)(-V_{dc} - i r - \omega_e i d L_s / d \theta_e) \\ &\quad + \omega_e i d L_m / d \theta_e \end{aligned} \quad (8)$$

where  $v_{mf}$  is the mutually induced voltage while the adjacent energized phase is operated in a free-wheeling mode. From equation (8), it is easy to understand that the voltage  $v_{mf}$  is always negative because the last term is small. As a result, we can design a rectifier circuit to change the polarity of the voltage  $v_{mf}$ . After the rectifier circuit process is completed, the induced voltage becomes a positive value, and is expressed as

$$\begin{aligned} v_{mr} &= (L_m / L_s)(V_{dc} + i r + \omega_e i d L_s / d \theta_e) - \\ &\quad \omega_e i d L_m / d \theta_e \end{aligned} \quad (9)$$

where  $v_{mr}$  is the signal of the rectified mutually induced voltage while its adjacent phase is operated in a free-wheeling mode. Observing the equations (7) and (9), the last three terms can be canceled by using a smoothing or averaging circuit. Many different circuits can provide this function. In this paper, a passive filter is designed to eliminate the high frequency harmonics and to smooth (average) the  $v_{mc}$  and  $v_{mr}$ . The voltage at the output of the filter can be expressed approximately as

$$\begin{aligned} v_{mo} &= (1/2)(v_{mc} + v_{mr}) \\ &= (L_m / L_s)V_{dc} \end{aligned} \quad (10)$$

where  $v_{mo}$  is the output voltage of the filter. The equation (10) is very attractive because the induced voltage at the output of the filter is only related to the input dc voltage of

the converter, and the self and mutual inductances of the SRM. In addition, these inductances are related to the rotor position of the SRM. The rotor position of the SRM, therefore, can be easily estimated by detecting the output voltage of the filter.

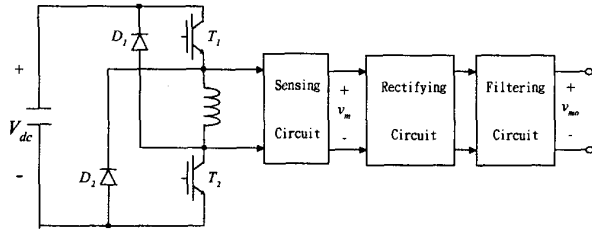


Fig. 1 The measuring and shaping circuit of the induced voltage.

### B. Sensorless Technique in the Single Pulse Region

By measuring the mutually induced voltage, we can obtain the estimating rotor position of an SRM. However, this method fails when the motor is operated at a high speed. After the motor reaches a high speed, the switching frequency of the PWM waveform is reduced. Finally, a single pulse current appears. Then, the equation (10) can not be applied. To solve this problem, a new method has been developed. This method uses the slope of the stator current to estimate the rotor position. The relationship between the exciting voltage and current is expressed as equation (6). From equation (6), we can easily obtain that

$$\frac{di}{dt} = [v_{ph} - ir - \omega_e idL_s / d\theta_e] / L_s \quad (11)$$

According to equation (11), after the self-inductance  $L_s$  increases, the phase current slope  $di/dt$  decreases. The relationship is shown in Fig. 2. According to Fig. 2, the slope of the phase current changes from a positive value to a negative value while the self-inductance increases. This means that the slope of the phase current is always larger for  $\theta_e \leq \theta_o$  than for  $\theta_e \geq \theta_o$ . As a result, we can detect the slopes of the three phase currents to estimate the rotor position when the motor is operated in a single pulse region [7].

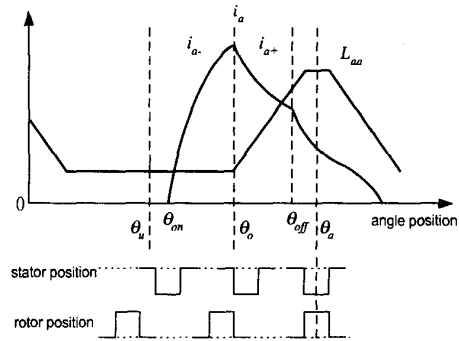


Fig. 2 The relationship between the phase current and the self-inductance.

### III. Implementation

The implementation of the proposed sensorless SRM drive system is shown in Fig. 3. The microprocessor system uses a Motorola 32-bit MC68020 CPU with a clock rate of 16.67 MHz. The CPU is equipped with a floating-point coprocessor, the MC68881. Therefore, all of the control methods can be computed using floating-point formats. The microprocessor can reside on a common VME bus with I/O ports, D/A converters, and A/D converters. The microprocessor system, as a result, is flexible. The MC68881 runs concurrently with the MC68020 to speed up the total required computation time.

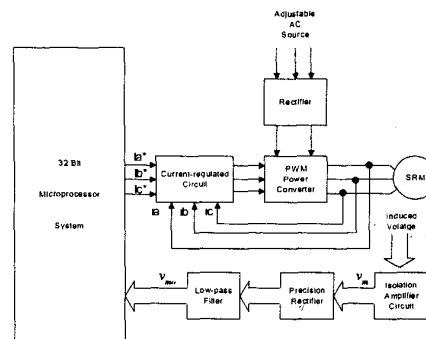
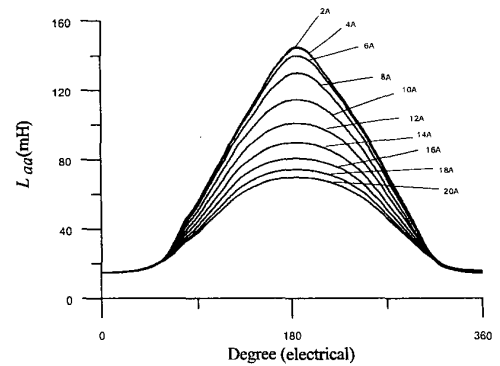


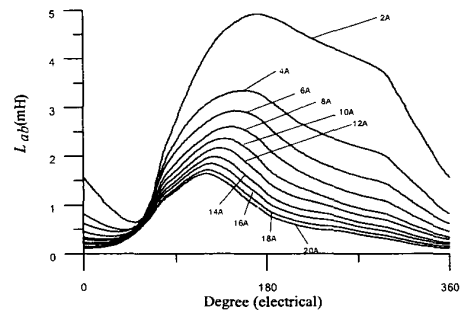
Fig. 3 The block diagram of the whole system.

#### IV. Experimental Results

Some experimental results are shown here. The SRM is coupled with a dynamometer, TM-5MT (DS), which is a product of the MEIWA company. The experimental waveforms are measured by a Tektronix digital storage oscilloscope-TDS 410. The parameters of the speed control are  $K_p=3$  and  $K_I=0.01$ . The input voltage of the converter is  $V_{dc}=150$  V. The inertia of the motor and dynamometer is  $0.025$  Nt-m-sec<sup>2</sup>/rad. The hysteresis band is set at  $\pm 0.3$  A. Some simulated and experimental results are shown here. Fig. 4(a) shows the measured inductance which is obtained by exciting the 2 A to 20A constant currents. Fig. 4(b) shows the measured mutual inductance which is obtained by exciting the 2 A to 20A constant currents. Fig. 5 shows the induced voltage waveform while the motor is operated at a PWM region. Fig. 5(a) is the measured a-phase voltage waveform that is detected at the output of the isolation amplifier circuit of the a-phase. Fig. 5(b) shows the waveform that has been processed by the rectifying and filtering circuits. In this figure, the waveform is a smoothing wave. Beyond 50 degrees, the signal is an induced voltage which is related to the rotor position. The setting voltage level and the signal cross at 150 degrees. At this point, the b-phase is blocked, and the c-phase is energized. As a result, we detect the a-phase induced voltage to determine the commutation time of turning off the b-phase and turning on the c-phase. Fig. 6 shows the rotor angles of the estimated angle and the real angle. The real angle is detected by using an encoder. Fig. 6(a) shows the measured real and estimated angles. Fig. 6(b) shows the estimating error. Fig. 7 shows the speed response of the system at a 30 r/min step input command. Fig. 8(a) shows the speed response of a 500 r/min step input command. Fig. 8(b) shows the load disturbance rejection response of the system at 500 r/min and 5 Nt-m. Fig. 9 shows the responses at 1200 r/min. Fig. 9(a) is the measured a-phase current. Fig. 9(b) is the measured a-phase sensed voltage. As you can see, it is reasonable to detect the slope change of the sensed voltage to obtain the instant of the slope change of the current. As a result, in this paper, the sensed voltage can be used to determine the angle  $\theta_o$ . Fig. 9(c) shows the transient response with at 1200 r/min.

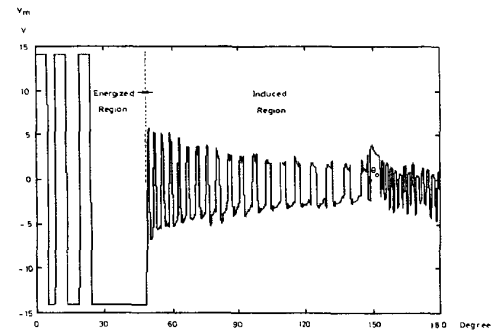


(a)

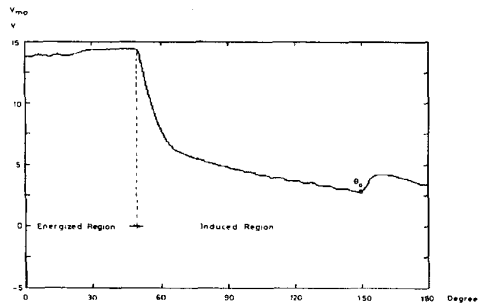


(b)

Fig. 4 The measured inductance (a) self inductance (b) mutual inductance



(a)



(b)  
 Fig. 5 The measured induced voltage (a) before rectifying  
 (b) after filtering.

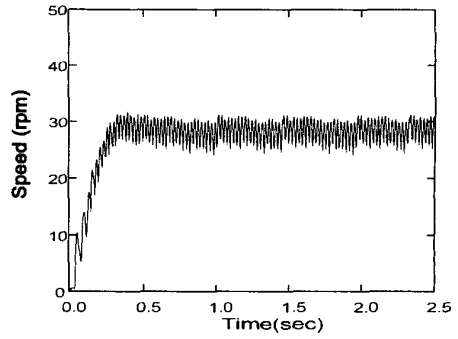
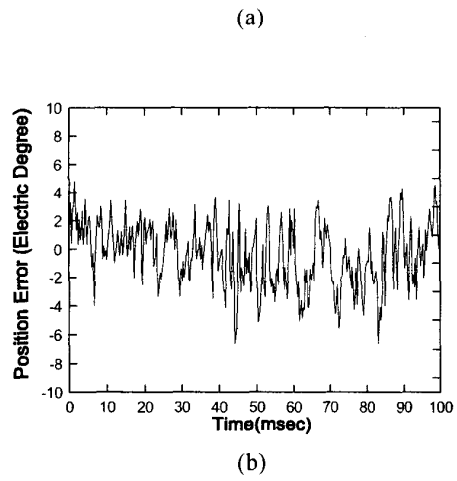
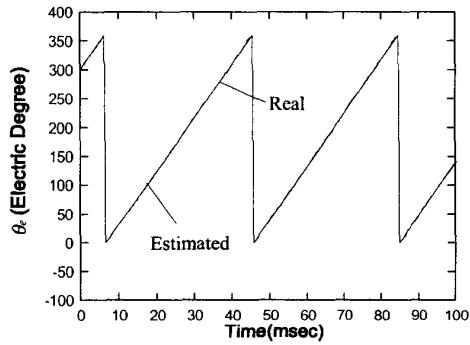
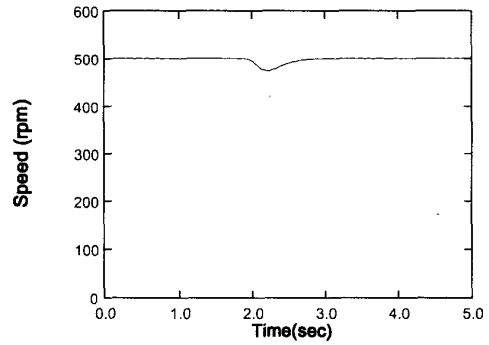
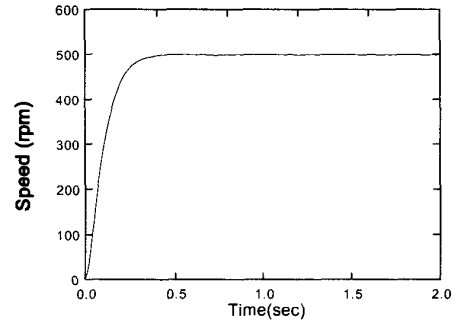


Fig. 7 The measured speed response of the sensorless drive  
 at 30 r/min.



(a)  
 (b)  
 Fig. 6 The estimated and real shaft angle  
 (a) angles (b) error



(a)  
 (b)  
 Fig. 8 The measured responses at 500 r/min  
 (a) transient response (b) load disturbance response.

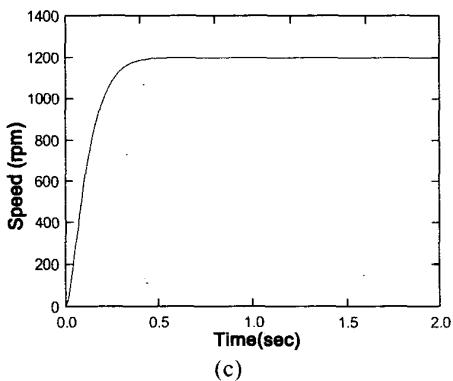
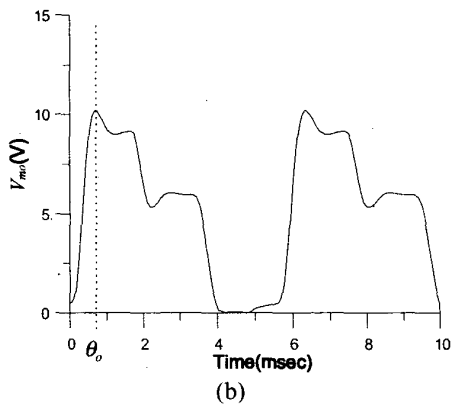
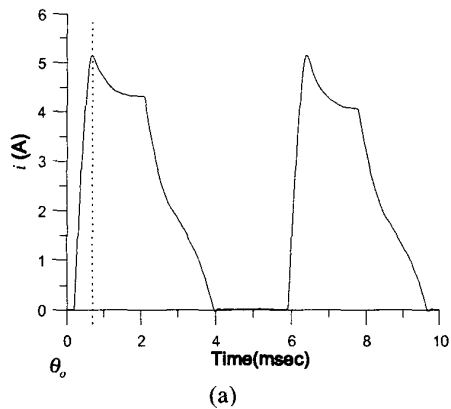


Fig. 9 The measured responses at 1200 r/min.  
 (a) a-phase current (b) a-phase sensed voltage  
 (c) transient response.

## V. Conclusions

In this paper, a simple technique to estimate the rotor position for a switched reluctance drive system has been presented. In addition, a microprocessor-based sensorless SRM drive has been implemented. The sensorless drive system performs well. Several experimental results show the feasibility and correctness of the proposed sensorless method. The methods proposed in this paper can easily be applied to actual industrial use due to its simplicity. This paper presents a new direction in the design of a sensorless switched reluctance drive system.

## References

- [1] T. A. Lipo, "Recent progress in the development of solid-state ac motor drives," *IEEE Trans. on Power Electron.*, vol. 3, no. 2, pp. 105-117, Apr. 1988.
- [2] B. K. Bose, "Power electronics and motion control-technology status and recent trends," *IEEE Trans. on Ind. Appl.*, vol. 29, no. 5, pp. 902-909, Sep./ Oct. 1993.
- [3] W. D. Harris and J. H. Lang, "A simple motion estimator for variable- reluctance motors," *IEEE Trans. on Ind. Appl.*, vol. 26, no. 2, pp. 237-243, Mar./Apr. 1990.
- [4] S. R. MacMinn, W. J. Rzesos, P. M. Szczesny and T. M. Jahns, "Application of sensor integration techniques to switched reluctance motor drives," *IEEE Trans. Ind. Appl.*, vol. 28, no. 6, pp. 1339-1343, Nov./Dec. 1992.
- [5] I. Husain, M. Ehsani, "Rotor position sensing in switched reluctance motor drives by measuring mutually induces voltages," *IEEE Trans. on Ind. Appl.*, vol. 30, no. 3, pp. 665-672, May/ June 1994.
- [6] B. Y. Ma, W. S. Feng, T. H. Liu, and C. G. Chen, "Design and implementation of a sensorless switched reluctance drive system," *IEEE Trans. on Aero. and Electron. System.*, vol. 34, no. 4, pp. 1193-1207, Oct. 1998.
- [7] G. G. Lopez, P. C. Kjar, and T. J. E. Miller, "A new sensorless method for switched reluctance motor drives," *Proc. IEEE-IAS'97*, pp. 564-570, New Orleans, Louisiana, Oct. 5-9, 1997.